Mesoporous SiO_2–TiO_2 epoxidation catalysts: tuning surface polarity to improve performance in the presence of water

Valentin Smeets, Lilia Ben Mustapha, Josefine Schnee, Eric M. Gaigneaux, Damien P. Debecker*

Institute of Condensed Matter and Nanosciences, Molecules, Solids, Reactivity (IMCN/MOST), Université catholique de Louvain, Place Louis Pasteur, 1, Box L4.01.09, 1348 Louvain-la-Neuve, Belgium.
*E-mail : damien.debecker@uclouvain.be Tel. : +32 10473648.

Abstract

Herein, we present the preparation by the non-hydrolytic sol-gel (NHSG) route of a mesoporous SiO_2–TiO_2 epoxidation catalyst with high specific surface area and large pores, and we discuss its modification by methylation. The pristine NHSG catalyst is tested for the catalytic conversion of cyclohexene with H_2O_2 in acetonitrile, showing performances comparable to a reference TS-1 catalyst. To expand the scope of the catalysts, we study their performance in the presence of water – present in aqueous solutions of H_2O_2, formed as a by-product of the epoxidation reaction, or used as a co-solvent. While TS-1 maintains high epoxidation activity, the pristine amorphous and mesoporous SiO_2-TiO_2 catalysts strongly deactivates when water s used as co-solvent. In order to circumvent this deactivation in the presence of water, we investigate the effect of surface hydrophobization with methyl groups on the catalytic activity and selectivity. Two functionalization methods are investigated: one-pot synthesis with methyltrichlorosilane and post-synthesis silanization with methyltrimethoxysilane. On the one hand, the one-pot methylation does not increase water resistance, in spite of an increased surface hydrophobicity. We interpret this result in the light of a poorer Ti dispersion and lower Ti^{4+} surface content in these catalysts. On the other hand, post-synthesis grafting was successful, allowing to maintain good epoxidation activity even in in the presence of water. This result is explained by a combination of a hydrophobic surface with a high active site content in this catalyst.

Keywords

Olefin epoxidation ; Mesoporous catalyst ; Non hydrolytic sol-gel ; Surface hydrophobicity ; Catalyst deactivation.

1. Introduction

Olefin epoxidation is widely represented in the chemical industry, from the production of pharmaceuticals to the polymer industry, due to the extensive use of these reactions for the synthesis of active intermediates (*e.g.* ethylene and propylene oxide, epichlorhydrin, cyclohexene oxide, etc.) [1]. With the recent advent of *green chemistry* and its associated principles [2], industrially relevant chemical processes, including olefin epoxidation, have to be re-designed. Sustainable routes are highly sought-for, not necessarily to maximize conversion or yield, but rather to minimize energy consumption and waste [3,4]. In the field of heterogeneous catalysis, this trend fosters the emergence of a new class of materials with relatively high activity and selectivity under mild conditions, *i.e.* in water-based media at moderately low temperatures [5,6].

Among the available catalysts and oxidants, the combination of titanium-containing zeolite TS-1 and hydrogen peroxide H_2O_2 represents one of the success-story of industrial epoxidation reactions. First, the efficiency of TS-1 in terms of catalytic activity and selectivity to epoxidation products, even at low temperatures and in the presence of water, stems for its success as an oxidation catalyst [7]. Second, H_2O_2 is commonly considered as one of the greenest oxidants, since it produces water as the only by-product. However, the atomic percentage of active sites in the MFI crystal structure is limited to a maximum of 2.5% (n Ti/ (n Ti + n Si)) [8]. Additionally, the intrinsic microporosity of TS-1 proscribes the use of this catalyst for the epoxidation of large olefins due to diffusional limitations. There is therefore a high demand for mixed oxides – either crystalline or amorphous – with larger pores and high surface area in order to extend the versatility of Ti-containing catalysts to a wider range of substrates [8–12]. Several challenges have to be addressed for the preparation of such materials, from the true incorporation of the active species (*i.e.* Ti^{4+}) by the levelling of the precursors reactivity (*e.g.* pre-hydrolysis of alkoxide precursors [13]) to the control over the texture by the choice of the templating agent, as well as proper drying conditions (*e.g.* supercritical drying [14]).

Sol-gel methods represent a versatile toolbox for the bottom-up preparation of heterogeneous catalysts [15]. Controlling the transition metal dispersion as well as the texture and functionalization of the catalyst surface, it is possible to obtain mesoporous silica-based epoxidation catalysts with high activity and selectivity. In particular, we put our focus on non-hydrolytic sol-gel (NHSG), which is currently emerging as a powerful preparation technique for mesoporous mixed oxide catalysts [16–19]. This approach allows reaching remarkable

specific surface area (*ca.* 1000 $m^2.g^{-1}$) and pore volume (*ca.* 1.0–1.5 $cm^3.g^{-1}$), associated with a tunable pore size and a high active phase dispersion without the need for organic templating agent, supercritical drying or pre-hydrolysis of the precursors [20,21]. In those conditions, catalysts with a high content of active sites can be obtained, with benefits for the catalytic performances compared to single TS-1 nanocrystals.

Despite the promising improvement brought by the fine control over the catalyst textural properties, amorphous SiO_2–TiO_2 mixed oxides are easily deactivated in water [22]. This issue has to be addressed when running epoxidation reactions with aqueous solutions of H_2O_2 (with concomitant production of H_2O) and/or in the presence of large amounts of water in the solvent.

An exception to deactivation by H_2O is provided by TS-1: its crystallinity and intrinsic hydrophobicity accounts for its good performance in aqueous media [22,23]. Increasing surface hydrophobicity of epoxidation catalysts was previously shown to be an pertinent strategy to increase the catalytic performance, when using H_2O_2 or organic peroxides as oxidant [24–30]. However, to the best of our knowledge, the improvement of the catalytic performance of amorphous titanosilicates in the presence of large amount of water by surface hydrophobization has not been addressed previously. Here, in order to circumvent the deactivation of the amorphous and mesoporous TiO_2–SiO_2 catalyst prepared by NHSG, we investigated the effect of surface hydrophobization on the catalyst activity using water as co-solvent for the epoxidation of cyclohexene. The surface functionalization was achieved either in one-pot during the gel synthesis or by post-synthesis silanization with a methylated precursor.

Not only the activity but also the selectivity is expected to be influenced by the surface hydrophobization. Considering the reaction pathway for cyclohexene oxidation (**Figure 1**), the epoxide can be produced by two competitive paths, either by *direct epoxidation* of cyclohexene with H_2O_2 or by the formation of cyclohexenyl hydroperoxide responsible for the oxidation of the olefin through a radical mechanism called *allylic oxidation* [22,26,31]. The second path should be avoided since it leads to the concomitant formation of undesired side products (2-cyclohexen-1-ol and its oxidation product 2-cyclohexen-1-one [32]). The mechanism implies the formation of a radical species on the Ti active site (*i.e.* TiO·) due to the over-adsorption of H_2O_2 onto the catalyst surface, which is favoured by a high H_2O_2/Ti ratio [26,33,34]. We put forward that increasing the surface hydrophobicity will locally reduce this ratio by repelling H_2O_2 molecules from the surface and thus from Ti active sites.

Consecutive to the formation of the epoxide, the ring opening of the epoxide to form a diol (cyclohexane diol) is another unwanted process (**Figure 1**). This hydrolysis reaction is promoted by the presence of H_2O [27,28] and therefore thought to be mitigated by surface

hydrophobization.

2. Experimental

The catalysts were prepared with a 6% at. Ti loading (Ti/Ti+Si) according to the non-hydrolytic sol-gel (NHSG) method, following a procedure described elsewhere [21]. Briefly, $SiCl_4$ (4.267 g, Acros Organics, 99.8%), $^{i}Pr_2O$ (5.449 g, Acros Organics, 99%) and $TiCl_4$ (0.304 g, Acros Organics, 99.9%) were successively transferred into a 100 cm^3 teflon-lined stainless steel autoclave along with CH_2Cl_2 (8.867 g, VWR Chemicals, 99.8%) in a glovebox. Prior to use, $^{i}Pr_2O$ and CH_2Cl_2 were dried using metallic sodium and P_2O_5, respectively, down to a water concentration below 15 ppm. The other reactants were used as received. The clear solution, with a molar composition of 1 $SiCl_4$: 0.064 $TiCl_4$: 2.127 $^{i}Pr_2O$: 4.165 CH_2Cl_2, was manually stirred for 10 min. The autoclave was subsequently sealed and kept in an oven at 150°C for 6 days. Afterwards, it was opened in the glovebox and the as-synthesized gel was ground and dried overnight under vacuum. The solid catalyst, in powder form, was obtained after calcination at 500°C for 5 h (10°C.min^{-1}). It is denoted "**NHSG**". As a reference material, titanosilicalite-1 (TS-1) was synthesized with a Ti atomic content of 1.8% [35].

One-pot functionalization. The gel was obtained by the same method as depicted above, but replacing part of the $SiCl_4$ by $MeSiCl_3$ (Sigma-Aldrich, 99%) [24]. The catalysts are denoted "**NHSG_XMe**", where "X" represents the nominal molar ratio $MeSiCl_3$/Si. The final composition was 1 $SiCl_4$: 0.111 $SiCl_3$: 0.071 $TiCl_4$: 2.309 $^{i}Pr_2O$: 4.628 CH_2Cl_2 (**NHSG_0.1Me)** and 1 $SiCl_4$: 0.429 $SiCl_3$: 0.091 $TiCl_4$: 2.825 $^{i}Pr_2O$: 5.950 CH_2Cl_2 (**NHSG_0.3Me)**.

Two-step functionalization. The pristine **NHSG** catalyst (200 mg) was methylated by a dry impregnation method using methyltrimethoxysilane (MTMS) (0.206 g, TCI, > 98%) in water-saturated toluene (0.062 g, Sigma-Aldrich, ≥ 99.7%). The impregnation solution was mixed with the solid sample and the mixture was further homogenised by vortexing for 10 min in a closed vial. Afterwards, the solid was put to rest in a toluene saturated atmosphere for 48 h. Then, the solid was heated at 90°C for 1 h, washed successively with 50 ml toluene and 50 ml pentane, and dried overnight at 120°C under vacuum. The nominal methylation ratio ($MeSi(OMe)_3$/Si) was 30%, and the catalyst is denoted "**NHSG@0.3Me**".

Textural properties were determined from N_2 adsorption/desorption isotherms at -196°C using a Tristar 3000 instrument (Micromeritics, USA). Prior to measurement, the samples were first degassed overnight under vacuum at 150°C. The pore size distribution was obtained from the desorption branch using the BJH method. The surface area was evaluated by the BET method in the relative pressure range of 0.05–0.30. Powder X-ray diffraction (PXRD) patterns

were recorded at room temperature on a Siemens D5000 diffractometer equipped with a Ni filter using CuKα radiation (Bragg-Brentano geometry) operated at 40 kV and 40 mA. Diffractograms were taken between 5° and 80° (2θ) with a step size of 0.02° (2θ). Diffuse reflectance spectra (DRS) were obtained with an AvaSpec-2048-1-DT (Avantes) spectrometer, equipped with a 300 lines/mm grating, a 100 μm slit size, a deuterium-halogen light source and a reflection probe with 6 illumination fibres and 1 read fibre. UV-visible spectra were recorded from 250 nm to 500 nm, with a 3 ms integration time of the CCD detector. Each spectrum was the average of 100 scans and smoothed using 3 pixels. The fluoropolymer Zenith® Ultrawhite (SphereOptics) was used as the white standard (> 99% reflectance). The Ti content of the materials was measured by ICP-AES on an ICP 6500 instrument (Thermo Scientific Instrument) after dissolution of the samples by sodium peroxide fusion. XPS experiments were carried out using an SSX 100/206 spectrometer (Surface Science Instruments, USA) with Al-Kα radiation operated at 10 kV and 20 mA. The Si 2p peak has been fixed to 103.5 eV to set the binding energy scale, in order to compensate for the possible different charging effects of organic and inorganic species [36]. The quantification of Ti in Ti–O–Si and Ti–O–Ti was based on the decomposition of the $2p_{3/2}$ peak at approximately 460.0 and 458.5 eV, respectively [37,38]. Si was quantified on the basis of the Si 2p peak at 103.5 eV. FT-IR spectra were collected in the ATR mode using an Equinox 55 spectrometer (Bruker) equipped with a Platinum ATR cell. The spectra were recorded between 4000 and 800 cm^{-1} with a resolution of 2 cm^{-1}. Each spectrum was the average of 100 scans. The organic content was determined by temperature-programmed oxidation (TPO) experiments carried out with a CATLAB-PCS (Hiden Analytical) instrument connected to a mass spectrometer. m/z = 15, 28, 29 and 44 were detected throughout the temperature program starting from 40°C to a final temperature of 800°C at a rate of 10°C/min. Surface hydrophobicity was evaluated from a water adsorption experiment by measuring the amount of water desorbed at 150°C under vacuum after 24 h storage in a humid environment [27].

The catalytic properties were investigated for the epoxidation of cyclohexene with hydrogen peroxide as the oxidizing agent. The reaction was carried out in a two-necked glass round-bottomed reactor at 60°C, equipped with a condenser, a magnetic stirrer and a rubber septum. In a typical run, 0.510 g (0.3 $mol.l^{-1}$) cyclohexene (Sigma-Aldrich, 99%), 0.092 g (0.05 $mol.l^{-1}$) toluene (Sigma-Aldrich, 99.7%) – used as the internal standard – and 120 mg (6 $g.l^{-1}$) catalyst were pre-mixed in 20 ml of AcN or AcN/H_2O 75:25 (v/v) under stirring. After 10 min, 0.136 g (0.06 $mol.l^{-1}$) of 30% (w/w) aqueous H_2O_2 was added and the mixture was allowed to react for 2 h. The product formation was followed by collecting aliquots at regular time intervals

and by analysing them in gas chromatography, using a Varian CP-3800 chromatograph equipped with a FID detector and a capillary column (BR-5, 30 m, 0.32 mm i.d., 1.0 μm film thickness).

3. Results and discussion

The elemental analysis of the xerogels showed that the experimental Ti content was in the 5.53–6.11 at.% (95% confidence interval), and thus very close to the nominal one (6 at.%). This result demonstrates a good control over the bulk composition for all the catalysts, with a quantitative incorporation of both titanium and silicon species in the final material. However, PXRD and DRS UV-vis analysis revealed the presence of small amounts of crystalline anatase TiO_2 phase in all samples (see Supplementary Information, **Fig. S1**). The presence of extra-framework TiO_2 is attributed to the difference of solvolysis-condensation rates around Si and Ti centres during the gel formation.

XPS analyses were conducted in order to investigate the surface composition and the quality of the Ti dispersion at the surface (**Table 1**). For NHSG, the surface Ti concentration matched the bulk content, showing that the synthesis method leads to homogeneous mixed oxides. Yet the Ti surface concentration is markedly lower than the bulk concentration when $MeSiCl_3$ is used as an additional precursor in the one-pot methylation procedure (**NHSG_0.1Me** and **NHSG_0.3Me**). This indicates a lack of homogeneity which was probably caused by different condensation rates of silicon and organosilicon precursors, as it is often reported for alkoxide precursors in sol-gel chemistry [39].

Among the Ti detected at the surface of the catalyst by XPS, one can distinguish the fraction that is truly incorporated into the silica matrix (denoted "Ti-O-Si" in **Table 1**) from the fraction that is not dispersed and instead present as TiO_2 inclusions. The former is found at 460.0 eV and the latter is found at 458.5 eV [37,38]. The decomposition of the Ti 2p peak of the catalysts is shown in **Figure S3** (Supplementary Information). In TS-1, as expected, almost all surface Ti atoms are incorporated in the well-defined crystalline titanosilicate matrix [40–42]. In the pristine **NHSG** catalyst, only a third of the surface Ti is in the highly dispersed form. This is consistent with the detection of small amounts of crystalline anatase by PXRD and DRS UV-vis. In the samples methylated via the one-step procedure, the amount of surface Ti is lower but the proportion of well-dispersed surface Ti atoms is higher.

N_2-physisorption isotherms are shown in **Figure 2**, along with the BJH pore size distribution. Textural data are summarized in **Table 2**. As expected, TS-1 solely displayed micropores and interparticular spaces which contribute to the total pore volume. In comparison, remarkably

high pore volumes and surface areas were obtained by the non-hydrolytic sol-gel method. **Figure 2** reveals the presence of mesopores with a distribution centred at *ca.* 9 nm in the pristine **NHSG** catalyst and in **NHSG@0.3Me**. On the opposite, the pore size distribution of **NHSG_0.1Me** shows small mesopores with diameter *ca.* 5 nm whereas **NHSG_0.3Me** does not present any pores above *ca.* 3.8 nm. The BET surface area is comparable for **NHSG** and the one-pot methylated catalysts **NHSG_0.1Me** and **NHSG_0.3Me**, whereas it is significantly lowered upon post-synthesis functionalization in **NHSG@0.3Me** (**Table 2**). Total pore volume is reduced by both methylation methods. The data indicate a lower impact of the post-synthesis grafting on the pore size, while decreasing both pore volume and surface area. Conversely, the one-pot methylation preserves the surface area while lowering the pore size and pore volume, which could be detrimental to the conversion of large molecules.

To probe the surface functionalization, the samples were analysed by FT-IR in ATR mode. The normalized spectra in the region 1300–900 cm^{-1} (**Fig. 3**) show the appearance of a vibration band at *ca.* 1280 cm^{-1} in **NHSG_0.1Me**, **NHSG_0.3Me** and **NHSG@0.3Me**. This band is characteristic of the Si–CH_3 stretching vibration (ν(Si–CH_3)) [43] and confirms the successful grafting of –CH_3 moieties in all the samples. The spectrum of **NHSG@0.3Me** displays a reduction of the Si–O^- stretching vibration band (ν(Si–O^-)) at *ca.* 950 cm^{-1}. Since this region is governed by the absorption of both Si–O–Ti and Si–OH groups [20,44], this observation evidences the grafting of the methyl groups through condensation reactions with surface silanols. The band at around 1060 cm^{-1} is attributed to the TO_1 (Transverse Optical) mode of Si–O–Si asymmetric stretching. The position of this band is affected by the stoichiometry (x) in SiO_x, which goes from 2 to 1.5 when switching from pure SiO_2 to $MeSiO_{1.5}$ [45]. For a functionalized surface, this peak is shifted to lower wavenumbers. This change of stoichiometry is only clearly visible for **NHSG_0.3Me**. The 20 cm^{-1} red shift observed for this catalyst indicates that the surface is indeed covered with methyl groups. The degree of methylation for **NHSG_0.1Me** and **NHSG@0.3Me** is probably too low to induce such shift in those cases.

The methyl content as well as the surface polarity have been approached by TPO and thermal analysis, respectively (**Table 3)**. Crystalline TS-1 is known to be more hydrophobic than amorphous xerogels [46]. This verifies in our study as **TS-1** indeed demonstrated a lower amount of adsorbed water than **NHSG** (**Table 3**). As expected, the presence of methyl groups correlated with a substantial decrease in the amount of water adsorbed on the solids, i.e. the higher the amount of methyl groups, the lower the adsorption of water. Interestingly, the **NHSG_0.1Me** and **NHSG@0.3Me** samples – prepared by different methods – appear to have a similar –CH_3 content and surface polarity.

The catalysts were tested in the epoxidation of cyclohexene at 60°C, first in AcN to verify their intrinsic epoxidation activity and then in an AcN/H_2O mixture (75:25 (v/v)) to test their resistance against water (**Table 4)**. A hot filtration test was carried out in AcN/H_2O 75:25 (v/v), confirming that all the catalytic activity was attributable to the solid material (see Supplementary Information, **Fig. S2**).

NHSG exhibits almost the same performances as the reference catalyst TS-1 in acetonitrile, whether expressed in yields or in TON (*Entries 1 and 2)*. Epoxide ring opening occurs to a moderate extent, as shown by a high % Epox. value (81–84%), which is typically obtained when an aqueous solution of H_2O_2 is used as the oxidant [27]. When the AcN/H_2O mixture was used as the solvent, TS-1 and NHSG catalysts behave very differently. On the one hand, the overall yield of TS-1 was barely affected (*Entry 3*), albeit the production of diol increased at the expense of the epoxide. This is expected in the presence of higher amount of H_2O which favours epoxide ring opening. On the other hand, a drastic loss of activity was observed for the **NHSG** catalyst (*Entry 4*). In that case, both the overall product yield and the epoxide yield are low; the epoxide yield drops to 2.1% only. The % DE value is approximately 50%, which is an indication that only the allylic oxidation routes is active and contributes to the formation of the epoxide [33].

This is attributed to the role played by water in the mechanism of direct epoxidation, as schematized in **Figure 4**. When H_2O adsorbs on the Ti active site, it hydrolyses one siloxane bridge, allowing titanium to release its internal tension by changing the coordination sphere from a tetrahedral to an octahedral configuration [22,47]. Classically, the coordination of a H_2O_2 molecule subsequently leads to the formation of the activated intermediate (*i.e.* Ti–OOH) that in turn oxidises the olefin via the direct epoxidation mechanism [40–42]. However, in amorphous materials such as **NHSG**, the system can undergo a second hydrolysis step that inactivates the complex and so prevents direct epoxidation. In crystalline TS-1, the formation of the inactive complex is hampered by the stable tripodal anchoring that maintains Ti–OOH in its activated form [22]; the latter is therefore available for direct epoxidation in the presence of the olefin. This partly explains the good performance of TS-1 even in the presence of water (*Entry 3*).

Nevertheless, it has been shown that tripodal Ti sites somehow favour the homolytic cleavage of the O–O bond of hydrogen peroxide compared to tetrahedral sites, thus leading to the formation of cyclohexenyl hydroperoxide (chhp, see **Fig. 1**) [32]. This explains the lower % H_2O_2 values for the catalysts tested in the presence of water, including TS-1, compared to acetonitrile.

The attractive performances of TS-1 in a water-containing medium, however, are also generally ascribed to the intrinsic hydrophobicity of this material [23]. On the one hand, hydrophobicity decreases the rate for epoxide ring opening, affecting positively the % Epox. value [27,28]. On the other hand, the unwanted allylic oxidation is known to be favoured by a high H_2O_2/Ti ratio (where "Ti" represents the amount of available Ti sites at the surface of the catalyst) [26,33,34]. Surface hydrophobicity provokes the repelling of H_2O_2 molecules from the surface thereby decreasing locally the H_2O_2/Ti ratio close to the active sites. This is proposed to explain the relatively high % DE values obtained with TS-1. Nevertheless, TS-1 is microporous, which limits its value in a range of potential applications.

Consistent with the foregoing, we aimed at stabilizing the mesoporous but amorphous NHSG catalysts by tuning surface hydrophobicity. The idea is to benefit from the advantageous open texture, while maintaining decent activity for the direct epoxidation in the presence of water (*Entries 5-7*, **Table 4**).

Despite its increased surface hydrophobicity, **NHSG_0.1Me** showed poor catalytic performance in AcN/H_2O (*Entry 6*), similar to the pristine **NHSG**. A possible explanation is linked to the capping of some Ti species by methyl groups during the gel formation (*i.e.* condensation of a $TiCl_4$ precursor with $MeSiCl_3$), resulting in a reduction of the amount of available active sites. Besides, the lack of homogeneity – resulting in a low concentration of dispersed surface Ti sites on the catalyst (see **Table 1**) and a high H_2O_2/Ti ratio (41 for **NHSG_0.1Me** *vs.* 31 for **NHSG**) – is another factor which could explain the low performance of this catalyst, despite the increased surface hydrophobicity. The situation is even worse for **NHSG_0.3Me** which has a three times higher methyl content but was totally inactive (**Table 3**). In this case, the lack of activity can be ascribed to the complete capping of the active sites by methyl groups, as evidenced by the strong shift of the TO_1 vibration band (1000-1100 cm^{-1}) in the FTIR-ATR spectrum of **NHSG_0.3Me**, and possibly to an excessive repelling of H_2O_2 from the surface or to possible diffusion issues within the smaller pores of this catalyst.

Compared to the pristine catalyst, **NHSG@0.3Me** shows the same total conversion (~13%) but a significant improvement in the epoxide yield (5.1% vs. 2.1% for the pristine **NHSG** catalyst). This is related to an increase in the % DE value up to 77%. As the yields of other co-products hardly varied, this result is a strong evidence of the re-activation of the *direct epoxidation* route. For this catalyst, the concentration of dispersed Ti active sites is thought to be unaffected by the methylation procedure due to the grafting of methyl groups through condensation with silanol groups. Therefore, we attribute the amelioration of the production of epoxide on **NHSG@0.3Me** to the repelling of H_2O and H_2O_2 molecules from the methyl-

grafted surface and so to the stabilization of the active sites for the direct epoxidation route. It should be noted that the epoxide yield is also beneficially affected by the lower tendency of this catalyst to promote ring opening. Yet, it is difficult to link this with an effect of hydrophobicity since **NHSG_0.1Me** – for which methylation has been successful and for which the water uptake was indeed lower, similar to **NHSG@0.3Me** – features a much lower value of % Epox.

4. Conclusions

Titanosilicates prepared by the NHSG method present high surface areas and pore volumes, combined with the presence of large mesopores which makes them very attractive for the conversion of bulky olefins such as cyclohexene. While highly active in organic solvent (AcN), the catalysts showed poor epoxidation activity in the presence of water. In those conditions, only the unwanted radical allylic oxidation route is active. In an attempt to restore the epoxidation efficiency of such amorphous catalyst, we proposed to increase their surface hydrophobicity.

Methyl groups were successfully incorporated in the xerogels, in one-pot, and this was shown to increase the surface hydrophobicity. However, these catalysts suffered from a lack of homogeneity, which resulted in a lower concentration of surface active sites. In the presence of water, the epoxide yield remained very low. Methylation by post-grafting, on the other hand, allowed to significantly restore the direct epoxidation mechanism, in the presence of water. In this case, the concentration of active sites remained the same and the surface hydrophobicity appears to protect the active site from the inactivating effect of water.

This study opens the way to the efficient use of amorphous and mesoporous titanosilicates for the epoxidation of large substrates in the presence of large amounts of water, allowing to simultaneously avoid deactivation and benefit from the open texture of such catalysts.

5. Acknowledgments

Authors acknowledge the ‘Communauté française de Belgique’ for the financial support – including the PhD fellowship of A. Vivian – through the ARC programme (15/20-069). F. Devred is acknowledged for the technical and logistical support. V. Smeets is thankful to F.R.S.–F.N.R.S for his FRIA PhD grant.

References

[1] M. Bohnet, Ullmann’s encyclopedia of industrial chemistry, Wiley-VCH, Weinheim, Germany, 2003.

[2] P. Anastas, N. Eghbali, Green Chemistry: Principles and Practice, Chem. Soc. Rev. 39

(2010) 301–312.

[3] R.A. Sheldon, Atom efficiency and catalysis in organic synthesis, Pure Appl. Chem. 72 (2000) 1233–1246.

[4] R.A. Sheldon, The e Factor: Fifteen years on, Green Chem. 9 (2007) 1273–1283.

[5] R.A. Sheldon, R.S. Downing, Heterogeneous catalytic transformations for environmentally friendly production, Appl. Catal. Gen. 189 (1999) 163–183.

[6] R.A. Sheldon, I.W.C.E. Arends, U. Hanefeld, Green Chemistry and Catalysis, 2007.

[7] B. Notari, Synthesis and Catalytic Properties of Titanium Containing Zeolites, Stud. Surf. Sci. Catal. 37 (1988) 413–425.

[8] Z. Kong, B. Yue, W. Deng, K. Zhu, M. Yan, Y. Peng, H. He, Direct synthesis of hierarchically porous TS-1 through a solvent-evaporation route and its application as an oxidation catalyst, Appl. Organomet. Chem. 28 (2014) 239–243.

[9] A. Taguchi, F. Schüth, Ordered mesoporous materials in catalysis, Microporous Mesoporous Mater. 77 (2005) 1–45.

[10] A. Corma, From microporous to mesoporous molecular sieve materials and their use in catalysis, Chem. Rev. 97 (1997) 2373–2419.

[11] M. Hartmann, A.G. Machoke, W. Schwieger, Catalytic test reactions for the evaluation of hierarchical zeolites, Chem. Soc. Rev. 45 (2016) 3313–3330.

[12] L.-H. Chen, X.-Y. Li, G. Tian, Y. Li, J.C. Rooke, G.-S. Zhu, S.-L. Qiu, X.-Y. Yang, B.-L. Su, Highly Stable and Reusable Multimodal Zeolite TS-1 Based Catalysts with Hierarchically Interconnected Three-Level Micro–Meso–Macroporous Structure, Angew. Chem. Int. Ed. 50 (2011) 11156–11161.

[13] C. Sanchez, J. Livage, M. Henry, F. Babonneau, Chemical modification of alkoxide precursors, J. Non-Cryst. Solids. 100 (1988) 65–76.

[14] G.M. Pajonk, Aerogel catalysts, Appl. Catal. 72 (1991) 217–266.

[15] D.P. Debecker, Innovative Sol-Gel Routes for the Bottom-up Preparation of Heterogeneous Catalysts, Chem. Rec. (2018) In Press. doi:10.1002/tcr.201700068.

[16] D.P. Debecker, P.H. Mutin, Non-hydrolytic sol–gel routes to heterogeneous catalysts, Chem. Soc. Rev. 41 (2012) 3624–3650.

[17] D.P. Debecker, V. Hulea, P.H. Mutin, Mesoporous mixed oxide catalysts via non-hydrolytic sol-gel: A review, Appl. Catal. Gen. 451 (2013) 192–206.

[18] A. Styskalik, D. Skoda, C.E. Barnes, J. Pinkas, The Power of Non-Hydrolytic Sol-Gel Chemistry: A Review, Catalysts. 7 (2017) 168.

[19] K. Bouchmella, M. Stoyanova, U. Rodemerck, D.P. Debecker, P. Hubert Mutin,

Avoiding rhenium loss in non-hydrolytic synthesis of highly active Re–Si–Al olefin metathesis catalysts, Catal. Commun. 58 (2015) 183–186.

[20] V. Lafond, P.H. Mutin, A. Vioux, Control of the Texture of Titania−Silica Mixed Oxides Prepared by Nonhydrolytic Sol−Gel, Chem. Mater. 16 (2004) 5380–5386.

[21] A.M. Cojocariu, P.H. Mutin, E. Dumitriu, F. Fajula, A. Vioux, V. Hulea, Mild oxidation of bulky organic compounds with hydrogen peroxide over mesoporous TiO2-SiO2 xerogels prepared by non-hydrolytic sol–gel, Appl. Catal. B Environ. 97 (2010) 407–413.

[22] M.G. Clerici, The activity of titanium silicalite-1 (TS-1): Some considerations on its origin, Kinet. Catal. 56 (2015) 450–455.

[23] R. Murugavel, H.W. Roesky, Titanosilicates: Recent Developments in Synthesis and Use as Oxidation Catalysts, Angew. Chem. Int. Ed. Engl. 36 (1997) 477–479.

[24] O. Lorret, V. Lafond, P.H. Mutin, A. Vioux, One-Step Synthesis of Mesoporous Hybrid Titania−Silica Xerogels for the Epoxidation of Alkenes, Chem. Mater. 18 (2006) 4707–4709.

[25] C. Swalus, B. Farin, F. Gillard, M. Devillers, E.M. Gaigneaux, Hybrid peroxotungstophosphate organized catalysts highly active and selective in alkene epoxidation, Catal. Commun. 37 (2013) 80–84.

[26] J.M. Fraile, J.I. García, J.A. Mayoral, E. Vispe, Silica-Supported Titanium Derivatives as Catalysts for the Epoxidation of Alkenes with Hydrogen Peroxide: A New Way to Tuneable Catalytic Activity through Ligand Exchange, J. Catal. 189 (2000) 40–51.

[27] R.L. Brutchey, D.A. Ruddy, L.K. Andersen, T.D. Tilley, Influence of surface modification of Ti-SBA15 catalysts on the epoxidation mechanism for cyclohexene with aqueous hydrogen peroxide, Langmuir ACS J. Surf. Colloids. 21 (2005) 9576–9583.

[28] D.A. Ruddy, R.L. Brutchey, T.D. Tilley, The Influence of Surface Modification on the Epoxidation Selectivity and Mechanism of TiSBA15 and TaSBA15 Catalysts with Aqueous Hydrogen Peroxide, Top. Catal. 48 (2008) 99–106.

[29] Z. Wang, K.J. Balkus Jr., Synthesis and modification of titanium containing wrinkled mesoporous silica for cyclohexene epoxidation, Microporous Mesoporous Mater. 243 (2017) 76–84.

[30] M.B. D'Amore, S. Schwarz, Trimethylsilylation of ordered and disordered titanosilicates: improvements in epoxidation with aqueous H2O2 from micro- to meso-pores and beyond†, Chem. Commun. 0 (1999) 121–122.

[31] E. Jorda, A. Tuel, R. Teissier, J. Kervennal, Synthesis, Characterization, and Activity in the Epoxidation of Cyclohexene with Aqueous H2O2of Catalysts Prepared by Reaction

of TiF4with Silica, J. Catal. 175 (1998) 93–107.

[32] A. Kumar, D. Srinivas, P. Ratnasamy, Synthesis of framework Ti-substituted, 3-D hexagonal, mesoporous Ti-SBA-12 for selective catalytic oxidation, Chem. Commun. 0 (2009) 6484–6486.

[33] J.M. Fraile, J.I. García, J.A. Mayoral, E. Vispe, D.R. Brown, M. Naderi, Is MCM-41 really advantageous over amorphous silica? The case of grafted titanium epoxidation catalysts, Chem. Commun. 0 (2001) 1510–1511.

[34] J.M. Fraile, J.I. García, J.A. Mayoral, E. Vispe, Effect of the Reaction Conditions on the Epoxidation of Alkenes with Hydrogen Peroxide Catalyzed by Silica-Supported Titanium Derivatives, J. Catal. 204 (2001) 146–156.

[35] A. Thangaraj, M.J. Eapen, S. Sivasanker, P. Ratnasamy, Studies on the synthesis of titanium silicalite, TS-1, Zeolites. 12 (1992) 943–950.

[36] M. Jacquemin, M.J. Genet, E.M. Gaigneaux, D.P. Debecker, Calibration of the X-Ray Photoelectron Spectroscopy Binding Energy Scale for the Characterization of Heterogeneous Catalysts: Is Everything Really under Control?, ChemPhysChem. 14 (2013) 3618–3626.

[37] B. Erdem, R.A. Hunsicker, G.W. Simmons, E.D. Sudol, V.L. Dimonie, M.S. El-Aasser, XPS and FTIR Surface Characterization of TiO2 Particles Used in Polymer Encapsulation, Langmuir. 17 (2001) 2664–2669.

[38] B.M. Reddy, B. Chowdhury, P.G. Smirniotis, An XPS study of the dispersion of MoO3 on TiO2–ZrO2, TiO2–SiO2, TiO2–Al2O3, SiO2–ZrO2, and SiO2–TiO2–ZrO2 mixed oxides, Appl. Catal. Gen. 211 (2001) 19–30.

[39] C.J. Brinker, G.W. Scherer, Sol-Gel Science: The Physics and Chemistry of Sol-Gel Processing, Academic Press, 2013.

[40] H. Munakata, Y. Oumi, A. Miyamoto, A DFT Study on Peroxo-Complex in Titanosilicate Catalyst: Hydrogen Peroxide Activation on Titanosilicalite-1 Catalyst and Reaction Mechanisms for Catalytic Olefin Epoxidation and for Hydroxylamine Formation from Ammonia, J. Phys. Chem. B. 105 (2001) 3493–3501.

[41] W. Panyaburapa, T. Nanok, J. Limtrakul, Epoxidation Reaction of Unsaturated Hydrocarbons with H2O2 over Defect TS-1 Investigated by ONIOM Method: Formation of Active Sites and Reaction Mechanisms, J. Phys. Chem. C. 111 (2007) 3433–3441.

[42] J. Stare, N.J. Henson, J. Eckert, Mechanistic Aspects of Propene Epoxidation by Hydrogen Peroxide. Catalytic Role of Water Molecules, External Electric Field, and Zeolite Framework of TS-1, J. Chem. Inf. Model. 49 (2009) 833–846.

[43] N.B. Colthup, L.H. Daly, S.E. Wiberley, Introduction to Infrared and Raman Spectroscopy, Third Edition, 3 edition, Academic Press, Boston, 1990.

[44] H. Chun, W. Yizhong, T. Hongxiao, Preparation and characterization of surface bond-conjugated TiO2/SiO2 and photocatalysis for azo dyes, Appl. Catal. B Environ. 30 (2001) 277–285.

[45] X. Landreau, B. Lanfant, T. Merle, C. Dublanche-Tixier, P. Tristant, A thorough FT-IR spectroscopy study on micrometric silicon oxide films deposited by atmospheric pressure microwave plasma torch, Eur. Phys. J. D. 66 (2012) 160.

[46] E.M. Flanigen, J.M. Bennett, R.W. Grose, J.P. Cohen, R.L. Patton, R.M. Kirchner, Silicalite, a new hydrophobic crystalline silica molecular sieve, Nature. 271 (1978) 512–516.

[47] C. Lamberti, S. Bordiga, D. Arduino, A. Zecchina, F. Geobaldo, G. Spanó, F. Genoni, G. Petrini, A. Carati, F. Villain, G. Vlaic, Evidence of the Presence of Two Different Framework Ti(IV) Species in Ti−Silicalite-1 in Vacuo Conditions: an EXAFS and a Photoluminescence Study, J. Phys. Chem. B. 102 (1998) 6382–6390.

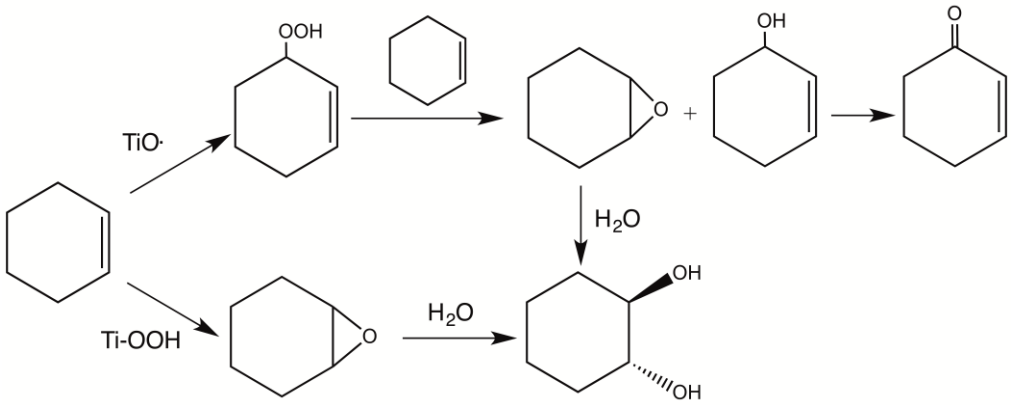

Figure 1. Reaction scheme for the epoxidation of cyclohexene via the *allylic oxidation* (up) or the *direct epoxidation* routes (bottom) [26].

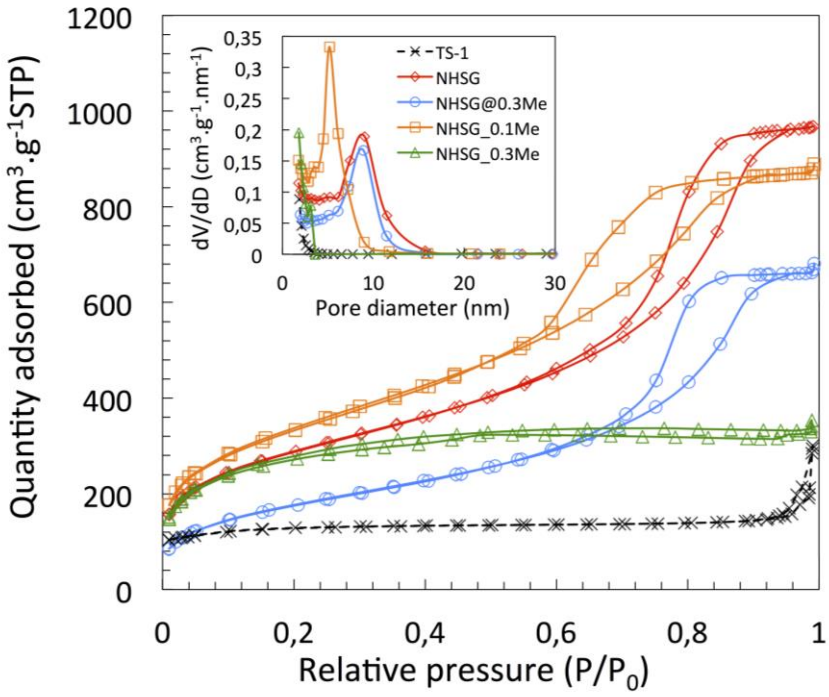

Figure 2. N_2 adsorption-desorption isotherms of the catalysts. Pore size distributions (PSD) based on the desorption branch are shown in inset.

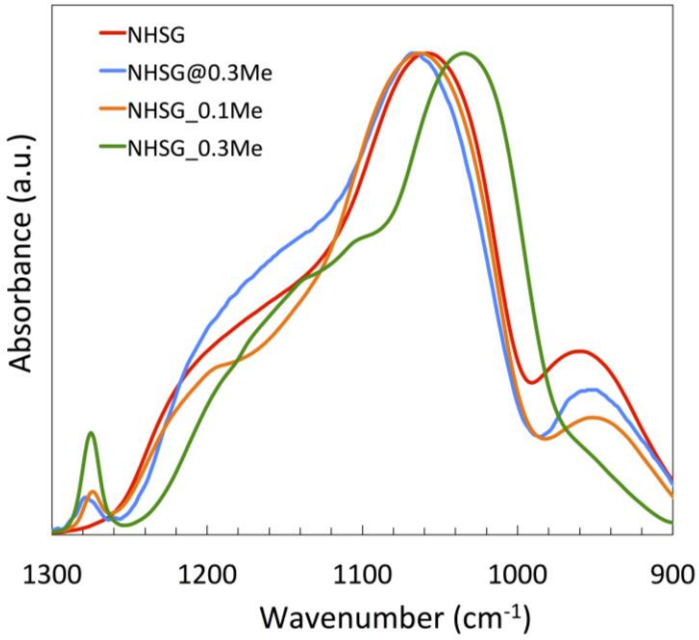

Figure 3. Normalized FT-IR spectra (ATR) of the methylated samples relative to the unmodified catalyst.

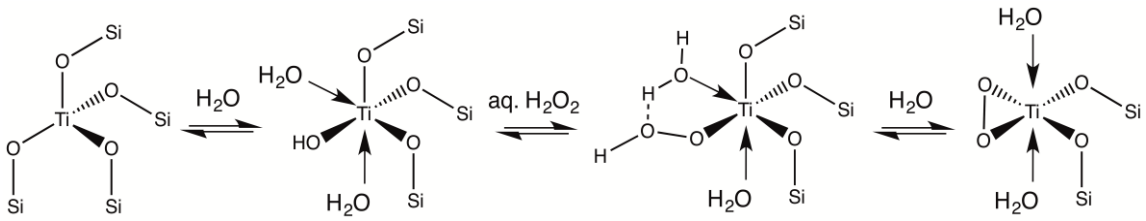

Figure 4. Mechanism of the inactivation of amorphous titanosilicate epoxidation catalysts in the presence of water.